








## Article

# Physicochemical and Morphological Study of the *Saccharomyces cerevisiae* Cell-Based Microcapsules with Novel Cold-Pressed Oil Blends

Wojciech Cichocki <sup>1</sup>, Adrian Czerniak <sup>2</sup>, Krzysztof Smarzyński <sup>1</sup>, Paweł Jeżowski <sup>3</sup> , Dominik Kmiecik <sup>1</sup> , Hanna Maria Baranowska <sup>4</sup> , Katarzyna Walkowiak <sup>4</sup> , Ewa Ostrowska-Ligeza <sup>5</sup> , Maria Barbara Różańska <sup>1</sup> , Mariusz Lesiecki <sup>1</sup> and Przemysław Łukasz Kowalczewski <sup>1,\*</sup> 

<sup>1</sup> Department of Food Technology of Plant Origin, Poznań University of Life Sciences, 60-624 Poznań, Poland; wojciech.cichocki@up.poznan.pl (W.C.); krzysztof.smarzynski@gmail.com (K.S.); dominik.kmiecik@up.poznan.pl (D.K.); maria.rozanska@up.poznan.pl (M.B.R.); mariusz.lesiecki@up.poznan.pl (M.L.)

<sup>2</sup> Center for Advanced Technologies, Adam Mickiewicz University in Poznań, 61-614 Poznań, Poland; adrcze@amu.edu.pl

<sup>3</sup> Institute of Chemistry and Technical Electrochemistry, Poznan University of Technology, 60-965 Poznań, Poland; pawel.jezowski@put.poznan.pl

<sup>4</sup> Department of Physics and Biophysics, Poznań University of Life Sciences, 60-637 Poznań, Poland; hanna.baranowska@up.poznan.pl (H.M.B.); katarzyna.walkowiak@up.poznan.pl (K.W.)

<sup>5</sup> Department of Chemistry, Institute of Food Sciences, Warsaw University of Life Sciences, 02-776 Warsaw, Poland; ewa\_ostrowska\_ligeza@sggw.edu.pl

\* Correspondence: przemyslaw.kowalczewski@up.poznan.pl



**Citation:** Cichocki, W.; Czerniak, A.; Smarzyński, K.; Jeżowski, P.; Kmiecik, D.; Baranowska, H.M.; Walkowiak, K.; Ostrowska-Ligeza, E.; Różańska, M.B.; Lesiecki, M.; et al. Physicochemical and Morphological Study of the *Saccharomyces cerevisiae* Cell-Based Microcapsules with Novel Cold-Pressed Oil Blends. *Appl. Sci.* **2022**, *12*, 6577. <https://doi.org/10.3390/app12136577>

Academic Editor: Alexandros Ch. Stratakos

Received: 14 June 2022

Accepted: 27 June 2022

Published: 29 June 2022

**Publisher's Note:** MDPI stays neutral with regard to jurisdictional claims in published maps and institutional affiliations.



**Copyright:** © 2022 by the authors. Licensee MDPI, Basel, Switzerland. This article is an open access article distributed under the terms and conditions of the Creative Commons Attribution (CC BY) license (<https://creativecommons.org/licenses/by/4.0/>).

**Abstract:** Vegetable oils rich in polyunsaturated fatty acids are a valuable component of the human diet. Properly composed oil blends are characterized by a 5:1 ratio of  $\omega 6/\omega 3$  fatty acids, which is favorable from a nutritional point of view. Unfortunately, their composition makes them difficult to use in food production, as they are susceptible to oxidation and are often characterized by a strong smell. Encapsulation in yeast cells is a possible solution to these problems. This paper is a report on the use of native and autolyzed yeast in the encapsulation of oils. The fatty acid profile, encapsulation efficiency, morphology of the capsules obtained, and thermal behavior were assessed. Fourier transform infrared analysis and low-field nuclear magnetic resonance relaxation time measurements were also performed. The process of yeast autolysis changed the structure of the yeast cell membranes and improved the loading capacity. Lower encapsulation yield was recorded for capsules made from native yeast; the autolysis process significantly increased the value of this parameter. It was observed that NY-based YBMCs are characterized by a high degree of aggregation, which may adversely affect their stability. The average size of the AY capsules for each of the three oil blends was two times smaller than the NY-based capsules. The encapsulation of oils in yeast cells, especially those subjected to the autolysis process, ensured better oxidative stability, as determined by DSC, compared to fresh blends of vegetable oils. From LF NMR analysis of the relaxation times, it was shown that the encapsulation process affects both spin-lattice  $T_1$  and spin-spin  $T_2^*$  relaxation times. The  $T_1$  time values of the YBMCs decreased relative to the yeast empty cells, and the  $T_2^*$  time was significantly extended. On the basis of the obtained results, it has been proven that highly unsaturated oils can be used as an ingredient in the preparation of functional food via protection through yeast cell encapsulation.

**Keywords:** yeast cells; microencapsulation; yeast cell walls; protection; yeast-based microcapsules; oxidative stability

## 1. Introduction

Fats and fatty acids are important nutrients that have a significant impact on growth and development at a young age but also have an impact on chronic nutrition-related

diseases later in life. Some of the fatty acids cannot be synthesized by humans and must therefore be obtained from the diet. These include polyunsaturated fatty acids (PUFA),  $\omega$ 6 linoleic acid (LA, 18:2  $\omega$ 6) from vegetable oils, and  $\omega$ 3  $\alpha$ -linolenic acid (ALA, 18:3  $\omega$ 3) from plant sources. PUFA  $\omega$ 3, eicosapentaenoic acid (EPA, 20:5  $\omega$ 3), and docosahexaenoic acid (DHA, 22:6  $\omega$ 3) can be found in fish and crustaceans. In the case of plant-based diets, the supply of these fatty acids is therefore severely limited. However, it is possible to synthesize DHA and EPA from ALA, as long as its supply is at a sufficient level [1].

Vegetable oils are obtained from the seeds of plants containing a minimum of 15% fat. Depending on the type of seed and their nutritional value and pressing ability, various technologies for obtaining oils are used, among which cold pressing is becoming more and more popular [2,3]. The use of low temperature during the entire process (40–50 °C) makes such oils a rich source of many nutrients, such as vitamins or biologically active compounds [4] but most of all, they provide monounsaturated (MUFA) and polyunsaturated fatty acids (PUFA) [5]. Cold-pressed oils are characterized by a specific, distinct taste and smell, and a greater possibility of auto-oxidation, i.e., spontaneous attachment of the O<sub>2</sub> molecule to unsaturated fatty acids, which causes them to become rancid more quickly [6]. Access to sunlight and oxygen are usually the main factors causing the oxidation of vegetable oils; this is due to the increased reactivity of methylene groups and unsaturated bonds [7,8]. Vegetable oils are also a frequent ingredient in recipes and are subjected to thermal treatment. Susceptibility to oxidation increases with the number of double bonds in fatty acid molecules. The more PUFAs in the oil, the greater the susceptibility to unfavorable changes or losses of valuable bioactive ingredients (tocopherols, polyphenols, sterols, phytosterols, squalene, carotenoids, and chlorophylls) when using high temperatures [9].

Oils available on the market are characterized by a different composition of polyunsaturated fatty acids. Very often, these products are characterized by a high  $\omega$ 6/ $\omega$ 3 acid ratio. Depending on the diet, this may have an adverse effect on human health. From a health point of view, the recommended optimal ratio of  $\omega$ 6/ $\omega$ 3 fatty acids ranges from 5:1 to 10:1 [10]. One of the ways to obtain the optimal  $\omega$ 6/ $\omega$ 3 ratio may be to mix oils and obtain blends with specific health properties [11]. The high content of unsaturated fatty acids is also one of the problems with the use of high nutritional oils in the production of foods subjected to cooking or foods with extended shelf life. As a result of food storage, fatty acids can be oxidized, and the formation of volatile compounds can significantly affect the deterioration of the sensory properties of food. During heating, oils are susceptible to oxygen in the air, water from the products (e.g., during frying), and the high temperature of the overall process. Consequently, they undergo changes in the processes of oxidation, hydrolysis, and polymerization [12]; thus, a number of compounds with different molecular weights are formed, which affect the health safety of food and its sensory acceptability [13,14].

Among the many methods of protecting fats against negative changes and degradation is the use of antioxidants that protect fatty acids against oxidation, e.g., synthetic (butylated hydroxytoluene-BHT, butylated hydroxyanisole-BHA, tert-butylhydroquinone-TBHQ, galates, natural tocopherols, and phenolic compounds obtained as an extract from different plants) [15], and also encapsulation, which allows for the protection of compounds against a potentially aggressive environment yet this also often releases them in an active form in certain places of the gastrointestinal tract. In addition to the commonly used encapsulation method in saccharide matrices (e.g., using maltodextrin) [16,17], yeast cells are also known for their ability to absorb large amounts of both hydrophobic and hydrophilic substances. Yeast-based microcapsules (YBMCs) significantly increase the oxidative stability of the active ingredient compounds encapsulated in them compared to the methods of traditional encapsulation in polysaccharide shells [18]. Both native yeast and yeast subjected to technological processes, improving their ability to bind active substances, can be used for the encapsulation process. The main techniques used to empty yeast cells are plasmolysis, autolysis, and enzymatic hydrolysis [19].

Cold-pressed oils contain significant amounts of MUFA, PUFA, but also other biologically active compounds, which makes them difficult to store and use in food production, especially during thermal processing. Bearing the aforementioned in mind, the aim of this study was to evaluate the possibility of using *S. cerevisiae* yeast cells as an encapsulating carrier for cold-pressed oil blends with a 5:1 ratio of  $\omega 6/\omega 3$  fatty acids to protect against adverse oxidative changes and in order to maintain high biological activity. To date, this method has not been used to protect oil blends with such a ratio of nutritionally important fatty acids. The obtained microcapsules were characterized in terms of their morphology and particle size distribution, but also their properties were examined using DSC, FT-IR, and low-field NMR techniques.

## 2. Materials and Methods

### 2.1. Oil Blends

Cold-pressed rapeseed, black cumin, wheat germ, evening primrose, and camelina oils, as well as refined rice bran oil, were used to obtain blends of oils which were further used for encapsulation. The oils were ordered directly from the oil producer (Semco Sp.z o.o. Sp.k., Smiřowo, Poland). Recipes of 16 blends were developed, the  $\omega 6/\omega 3$  fatty acid composition of which was characterized by a ratio of 5:1. The composition of the oil blends was developed at the earlier stages of the research project and was submitted for patent protection [20,21]. Cold-pressed oils were used due to the higher content of antioxidants, including phenolic compounds. In this study, three oil blends were used (Table 1), which in previous studies were characterized by high biological activity [11], in order to protect them during storage and use in food production.

**Table 1.** Composition of oil blends.

Code	Type of Oil			Share (%)		
RBWg	Rapeseed oil	Black cumin oil	Wheat germ oil	50	30	20
REp	Rapeseed oil	Evening primrose oil		65	35	-
CRb	Camelina oil	Rice bran oil		12	88	-

### 2.2. Fatty Acid Composition

The fatty acid composition was determined according to the AOCS Official Method Ce 1h-05 [22] using an Agilent 7820A GC equipped with a flame ionization detector (FID) (Agilent Technologies, Santa Clara, CA, USA). The oil samples were first dissolved in *n*-hexane and transesterified with sodium methylate. After transesterification, the fatty acid methyl esters (FAME) were separated using the SLB-IL111 capillary columns (Supelco, Bellefonte, PA, USA) (100 m, 0.25 mm, 0.20 mm).

### 2.3. Baker's Yeast Cell Pretreatment

In order to remove residue of the culture medium and cell fragments, purchased in a store, commercially available *Saccharomyces cerevisiae* baker's yeast (Lesaffre Polska S.A., Wolczyn, Poland) was rinsed three times with 0.01 M phosphate buffer [23]; the buffer to yeast ratio was 5:1. Each time the obtained yeast suspension was centrifuged (20 min, 3500 × *g*) in order to separate the biomass, and then the buffer was decanted. After the final rinsing and centrifugation, the yeast was frozen (−22 °C), freeze-dried, and ground using a laboratory grinder. The obtained native yeast (NY) from this process was further used for the encapsulation process.

In order to maximize the capacity of yeast shells, the washed NY wet biomass was subjected to autolysis. First, the pH of the yeast suspension was adjusted to 5.5 with 0.5 N HCl. It was then incubated for 48 h at 55 °C in a water bath with stirring set at 150 rpm [24]. After this time, the yeast was rinsed five times with 0.01 M phosphate buffer, centrifuged (20 min, 3500 × *g*), frozen, and freeze-dried. Autolyzed yeast, denoted as AY, was used then for the encapsulation process.

#### 2.4. Microencapsulation

The microencapsulation of the oil blends (according to Table 1) in yeast biomass was carried out based using the methodology used by Czerniak et al. [24], with a few modifications as described in the Polish patent application [25]. The microencapsulation was carried out in triplicate for two parallel tests ( $n = 6$ ). The binding of oil with biomass (both NY and AY) was carried out in glass bottles with a capacity of 250 mL, with an amount of 40 g of deionized water containing 3% wt. addition of the emulsifier Tween 80 (polyoxyethylene sorbitan monooleate). Then, 10 g of the blend of oils was added to the solution and homogenized (CAT X120 homogenizer with TN10 tip, Ingenieurbüro CAT, M. Zipperer GmbH, Ballrechten-Dottingen, Germany) for 5 min at  $16,000 \text{ min}^{-1}$  to prepare a pre-emulsion. The final emulsion was prepared with an ultrasonic homogenizer (Sonoplus HD 3200 with probe VS 70/T, BANDELIN electronic GmbH & Co. KG, Berlin, Germany), using the following process parameters: homogenization time 5 min, pulse length 20 s, pause 10 s, ultrasound frequency 10 kHz, and power 200 W with an amplitude of  $150 \mu\text{m}$ . During the homogenization, the vessel was cooled in an ice bath to limit the temperature increase, which during the entire emulsion formation process did not exceed  $35 \text{ }^\circ\text{C}$ . The mixture was incubated in a shaker (New Brunswick™ Excella E24, Eppendorf SE, Hamburg, Germany) with  $180 \text{ min}^{-1}$  agitation for 8 h at  $45 \text{ }^\circ\text{C}$ . After incubation, the contents of the vessels were poured into falcon tubes and centrifuged at  $3500 \times g$  (Rotina 380R, Andreas Hettich gmbH & Co. Kg, Tuttlingen, Germany) for 10 min to separate the biomass. The separated mass of microcapsules was then washed three times with deionized water to remove the remnants of the mixture. The wet biomass was transferred to lyophilization vessels and frozen at  $-20 \text{ }^\circ\text{C}$  for 12 h, and then freeze-dried at a pressure of 0.125 mbar for min. 48 h. The microcapsules prepared in this way were stored at  $-20 \text{ }^\circ\text{C}$  until analysis.

#### 2.5. Determination of Oil Content

An amount of 15 g of microcapsules was weighed into a filter paper thimble, which was then sealed with cotton wool and placed in a Soxhlet extractor. Extraction was performed with 200 mL of petroleum ether at the reflux temperature of the solvent for 2 h. After extraction, the oil-containing extract was transferred to a pre-weighed dry round bottom flask, and the solvent was evaporated using a vacuum rotary evaporator (BÜCHI Labortechnik AG, Flawil, Switzerland) at  $40 \text{ }^\circ\text{C}$  and 200 mbar, and then dried in a laboratory oven for 30 min at  $95 \text{ }^\circ\text{C}$ . Total oil content was calculated from the weight difference between the flask containing the oil and the dry flask.

#### 2.6. Encapsulation Yield (EY)

The EY was calculated according to formula:

$$EY [\%] = \frac{M_{OB}}{M_{MC}} \times 100$$

where:  $M_{OB}$ —the mass of the total oil encapsulated in yeast shells, and  $M_{MC}$  is the mass of the capsules.

#### 2.7. Microcapsule Morphology and Size

The morphology of the microcapsules was evaluated using a scanning electronic microscope (SEM) (Zeiss EVO 40, Carl Zeiss AG, Oberkochen, Germany). The size distribution of the microcapsules was measured using a Mastersizer 2000 (Malvern Panalytical GmbH, Herrenberg, Germany) using isopropanol as the dispersion medium.

#### 2.8. Fourier Transform Infrared (FT-IR) Spectroscopy

FT-IR spectra were obtained via a spectrophotometer of the Perkin Elmer company (Waltham, MA, USA), equipped with an ATR device with diamond as the internal reflection element [26]. Data were collected over a spectral range of  $4000\text{--}400 \text{ cm}^{-1}$ .

### 2.9. Melting Characteristic

DSC measurements of the melting characteristics of the oils were carried out with a TA DSC Q200 (TA Instruments Corporate, New Castle, DE, USA). Calibration was done with indium standards. Fat samples of 3–4 mg were placed into aluminum pans with a lid and were hermetically sealed. An empty sealed aluminum pan was used as a reference and the experiments were performed under a nitrogen atmosphere at normal pressure. Melted samples were heated to 80 °C and held for 10 min in order to melt all the crystals and to erase the thermal memory. The samples were then cooled to –80 °C at 10 °C/min and maintained at –80 °C for 30 min. Then the melting profiles were obtained by heating the samples to 80 °C at a heating rate of 15 °C/min [27].

### 2.10. Differential Scanning Calorimetry (DSC) Studies

The lyophilized capsules were studied by DSC (TA DSC Q 200, TA Instruments Corporate, New Castle, DE, USA) in a normal pressure cell. The cell was purged with dry nitrogen at 50 mL/min and calibrated for the baseline of an empty oven temperature using standard pure indium. Specific heat capacity was calibrated using a sapphire. The powders were cooled with a mechanical refrigeration cooling system (intracooler). An empty hermetically sealed aluminum pan was used as a reference in every test. The powders (10–15 mg) were hermetically sealed in aluminum pans (volume 30 µL). The samples were heated from –80 °C up to 200 °C with a heating rate of 5 °C/min. The DSC technique was used to obtain curves of heat flow (W/g) versus temperature curves [28].

### 2.11. Water Activity

Measurements of water activity were performed using an analyzer of water diffusion and activity ADA-7 (COBRABID, Poznań, Poland), with a system of automatic time recordings of the water evacuation runs from individual samples. The process was carried out for six repetitions ( $n = 6$ ). Detailed characteristics of the experimental method were performed as described by Le Thanh-Blicharz et al. [29]. Before the measurement, the chamber was dried to a water activity of 0.05. The temperature was stabilized at  $20.0 \pm 0.1$  °C using Peltier modules. The duration of one measurement was set at 1000 s.

### 2.12. Low-Field Nuclear Magnetic Resonance (LF NMR) Measurements

Measurements of relaxation times were performed using a pulse NMR spectrometer PS15T, operating at 15 MHz under a system-controlled temperature (Ellab, Poznań, Poland). The pulse sequence (180-t-90) [30] was applied for measurements of the spin-lattice relaxation times. Distances between RF pulses ( $t$ ) were changed within the range from 0.1 to 120 ms, and the repetition time was approximately 13 s. Each time, 32 FID signals and 100 points from each FID signal, were collected.

Five accumulation signals were employed. All samples were measured at  $20.0 \pm 0.5$  °C. All presented results are mean values and standard deviations, recorded from five repetitions of each sample.

Calculations of the spin-lattice relaxation time values were performed with the assistance of the CracSpin program [31], designed for calculating relaxation parameters from experimental data using the “spin grouping” approach. The Marquardt method of minimization was applied for fitting multiexponential decays. Standard deviation was used to determine the accuracy of the relaxation parameter measurement. Time changes of the current value from the FID signal amplitude used in the employed frequency of impulses are described by the following formula:

$$M_z = M_0 \left( 1 - 2e^{-\frac{t}{T_1}} \right)$$

where:  $M_0$  and  $M_z$  were equilibrium and accuracy magnetization amplitude, respectively.



### 2.13. Statistical Analyses


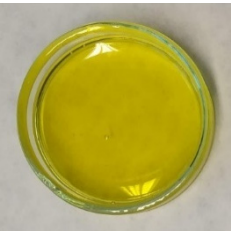
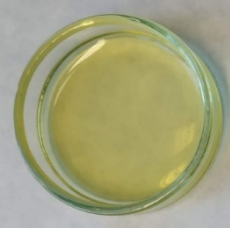
All measurements were repeated in triplicate, unless otherwise stated. Statistica 13 software (Dell Software Inc., Round Rock, TX, USA) was used to perform a one-way analysis of variance (ANOVA). A post-hoc Tukey HSD multiple comparison test was used to identify statistically homogeneous subsets at  $\alpha = 0.05$ .

## 3. Results and Discussion

### 3.1. Oil Blends Characteristics

The main determinant of the quality, nutritional value, and oxidative stability of edible oils is their fatty acid profile. Table 2 shows the percentage of fatty acid composition of the tested oil blends, as well as photographs of their color. It can be seen that both RBWg and REp were yellow, with the RBWg's color appearing much more intense (darker). CRb was characterized by a straw color. Chromatographic analysis of the fatty acid profile showed that the  $\omega 6/\omega 3$  fatty acid ratios were 5.05, 5.11, and 5.11 for RBWg, CRb, and REp, respectively. The fatty acids from  $\omega 3$  and  $\omega 6$  groups are extremely important for the proper development of the body, but from a nutritional point of view, the most important thing is their relationship to each other because both these groups of essential fatty acids compete for the same enzymes during metabolic processes in the human body [32]. Consuming excessive amounts of  $\omega 6$  fatty acids promotes inflammation, which in turn can lead to a wide variety of health conditions, including heart disease [33]. The WHO/FAO has suggested an optimal  $\omega 6/\omega 3$  ratio range from 5:1–10:1 [10].

**Table 2.** Fatty acid composition (%) and  $\omega 6/\omega 3$  fatty acid ratios of oil blends.

Fatty Acid	RBWg	REp	CRb
			
C16:0	9.36 ± 0.01 <sup>a</sup>	5.01 ± 0.23 <sup>b</sup>	15.55 ± 0.25 <sup>c</sup>
C16:1	0.19 ± 0.03 <sup>a</sup>	0.11 ± 0.01 <sup>a</sup>	0.13 ± 0.01 <sup>a</sup>
C18:0	1.89 ± 0.02 <sup>a</sup>	2.66 ± 0.06 <sup>b</sup>	1.65 ± 0.07 <sup>a</sup>
C18:1	42.79 ± 1.38 <sup>a</sup>	42.76 ± 1.15 <sup>a</sup>	37.14 ± 0.68 <sup>b</sup>
C18:2	37.19 ± 1.11 <sup>a</sup>	38.16 ± 0.22 <sup>a</sup>	36.71 ± 0.95 <sup>a</sup>
C18:3	7.37 ± 0.17 <sup>a</sup>	7.49 ± 0.68 <sup>a</sup>	7.18 ± 0.14 <sup>a</sup>
C20:0	0.11 ± 0.01 <sup>b</sup>	0.05 ± 0.01 <sup>a</sup>	0.69 ± 0.02 <sup>c</sup>
C20:1	1.02 ± 0.05 <sup>b</sup>	3.75 ± 0.08 <sup>c</sup>	0.57 ± 0.03 <sup>a</sup>
C22:0	0.02 ± 0.01 <sup>a</sup>	0.02 ± 0.01 <sup>a</sup>	nd
C22:1	0.06 ± 0.01 <sup>a</sup>	nd	0.39 ± 0.03 <sup>b</sup>
SFA	11.38 ± 0.01 <sup>b</sup>	7.73 ± 0.16 <sup>a</sup>	17.89 ± 0.34 <sup>c</sup>
MUFA	44.06 ± 1.30 <sup>b</sup>	46.61 ± 1.06 <sup>b</sup>	38.23 ± 0.75 <sup>a</sup>
PUFA	44.56 ± 1.28 <sup>a</sup>	45.66 ± 0.90 <sup>a</sup>	43.89 ± 1.09 <sup>a</sup>
$\omega 6/\omega 3$	5.05 ± 0.03 <sup>a</sup>	5.11 ± 0.44 <sup>a</sup>	5.11 ± 0.03 <sup>a</sup>

Composition of blends as shown in Table 1. Values are means of three determinations ± SD. Means in the same row followed by different letters indicate significant differences ( $p < 0.05$ ) between samples of each type of oil blend. nd—not detected. SFA—saturated fatty acid, MUFA—monounsaturated fatty acid, PUFA—polyunsaturated fatty acid.

All analyzed blends were characterized by a favorable nutritional profile of fatty acids with approximately a 90% proportion of unsaturated fatty acids and a range of only 7.73% (for CRb) to 17.89% (for REp) of saturated acids. The main SFA was palmitic acid, and there were also stearic, arachidic, and decanoic acids present. In the group of unsaturated fatty acids, the dominant compound was oleic acid (C18:1). The total share of this fatty

acid ranged from 37.14 to 42.79% for CRb and RBWg blends, respectively. The C18:2 *n*-6  $\alpha$ -linoleic acid dominated among the PUFAs, but the C18:3 *n*-3 (ALA) acid, which was also present in the analyzed blends, was more important from a nutritional point of view. ALA is not synthesized by the human body, it must be supplied by a person's diet, and it is necessary for the proper functioning of the body [34,35]. Moreover, ALA is a precursor in the *n*-3 fatty acid metabolic pathway, allowing the synthesis of eicosapentaenoic acid (EPA, 20:5) and docosahexaenoic acid (DHA, 22:6) in the organism [36,37]. The main sources of DHA and EPA are fish and seafood, which are eliminated in plant-based diets. However, ensuring an adequate level of DHA and EPA is crucial as the deficiency of these fatty acids can cause many adverse health effects [38–40].

### 3.2. Effect of Pretreatment on the Capacity of YBMCs

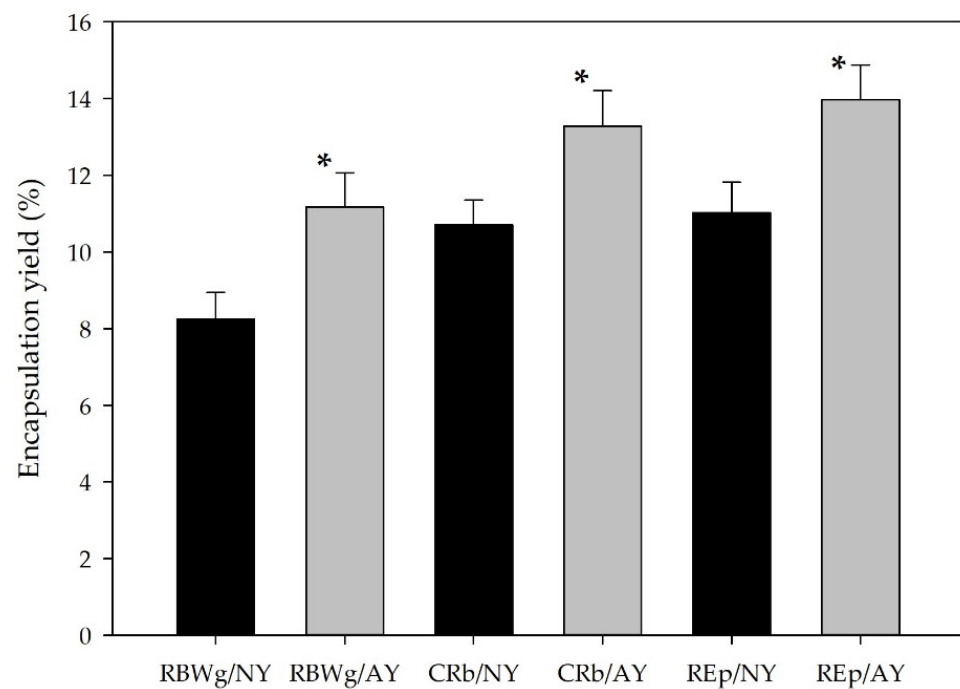
Both native *S. cerevisiae* yeast and autolyzed yeast were used in the present study to obtain YBMCs with oil blends with a nutritionally favorable fatty acid ratio. A significantly ( $p < 0.05$ ) higher increase in EY was observed in YBMCs obtained from autolyzed yeast compared to capsules based on native yeast (Figure 1). The structure of the cell wall determines its permeability; in NY, the passive transport was much slower hence the observed lower oil loading yield [41]. The biggest difference was observed in the case of RBWg encapsulation, and EY increased in AY versus NY by about 35.46%. Bishop et al. [42] indicate in their work that the encapsulation of oils in yeast cells is a process consisting of two sub-processes: releasing the yeast cell components into the reaction environment and the simultaneous extraction of oil from the environment, immobilized inside the cell. Shi et al. [23] indicate that the pre-treatment of yeast biomass by means of plasmolysis may result in an increase in encapsulation yield by as much as 50%. However, other authors in the published report indicated that cell plasmolysis did not result in a significant increase in the oil loading into capsules [19]. The calculated EY ranged from 8.25 to 13.98%, depending on the oil blend used. This may result from the conditions of the encapsulation process carried out in the aquatic environment. The high water content causes the walls of yeast cells to become hydrophilic due to the polysaccharides present in them, which limits the process of diffusion of hydrophobic molecules into the cells [43]. Nevertheless, Shi et al. [44], in their studies, showed similar EY values using yeast as an encapsulation carrier. In other studies, however, Pham-hoang et al. [45] showed that EY can be as high as 55%, depending on the encapsulated material.

### 3.3. YBMCs Morphology

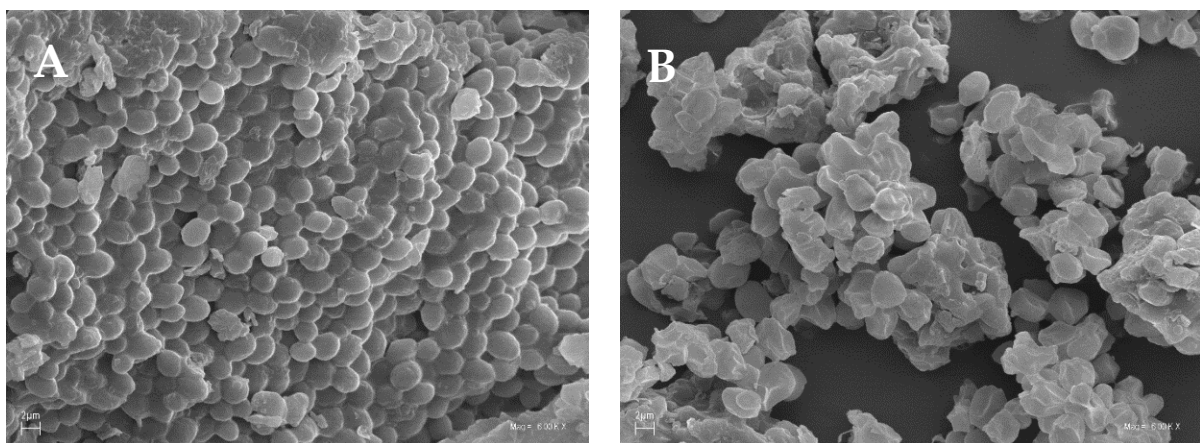
Figure 2 presents SEM pictures of the NY and AY microstructures, as well as YBMCs obtained from them from each of the 3 oil blends. Micrograph analysis showed significant morphological differences between the yeast cells without oil charged inside and the final microcapsules. Strong aggregation of NY cells was observed (Figure 2A), which was characterized by an oval, bubble-like shape. After the autolysis process, irregularly shaped collapsed bubbles were formed (Figure 2B). After the encapsulation process, the resulting capsules were mostly spherical, with the exception of RBWg/NY and REp/NY, whose shape was irregular. Literature data show that the aggregation of yeast cells is caused by a high content of  $\beta$ -glucans [46]. A strong agglomeration of microcapsules was also observed, especially in the case of NY capsules. Also, Czerniak et al. [24] observed similar agglomeration behavior for fish oil containing YBMCs. The reduction of YBMCs agglomeration due to cell autolysis increased the outer surface of the microcapsules and, consequently, the encapsulation efficiency. Therefore, preventing the aggregation of yeast cells in order to increase the diffusion rate of the encapsulated material into the YBMCs is recommended.

The size of yeast shells is important and determines their stability and microencapsulation efficiency. Small sized capsules are preferred as these make it easier to ensure uniformity and quality in food products [47]. The size distribution of YBMCs is presented in Table 3. The NY has uniform particle size distribution, as well as the obtained microcap-

sules (shown on Figure 3A). There is a noticeable shift towards higher values of the particle size distribution increasing after the absorption of oil during the encapsulation. In case of the AY, there is no uniformity in the particle size distribution. There is a wide range of different sizes of particles with local maxima (shown in Figure 3B). The autolysis process causes the removal of inside organelles from yeast cells and their partial disintegration, which can explain this characteristic of two sets of particle size distribution. Furthermore, autolysis does not impact every cell in the same way and usually leads to the limitation of cells aggregating and a more representative particle size distribution. On the other hand, the NY and NY-based microcapsules form aggregates (proven by SEM images), which can explain two separate maxima in the case of the AY samples and the uniform distribution of NY. Larger YBMCs provide better protection for the encapsulated material, but dissolve less well in the end products [48]. It has also been shown that the presence of large particles may be undesirable in most food products [49]. Capsules that are too small, however, can be empty containers that do not contain the encapsulated material inside [48].

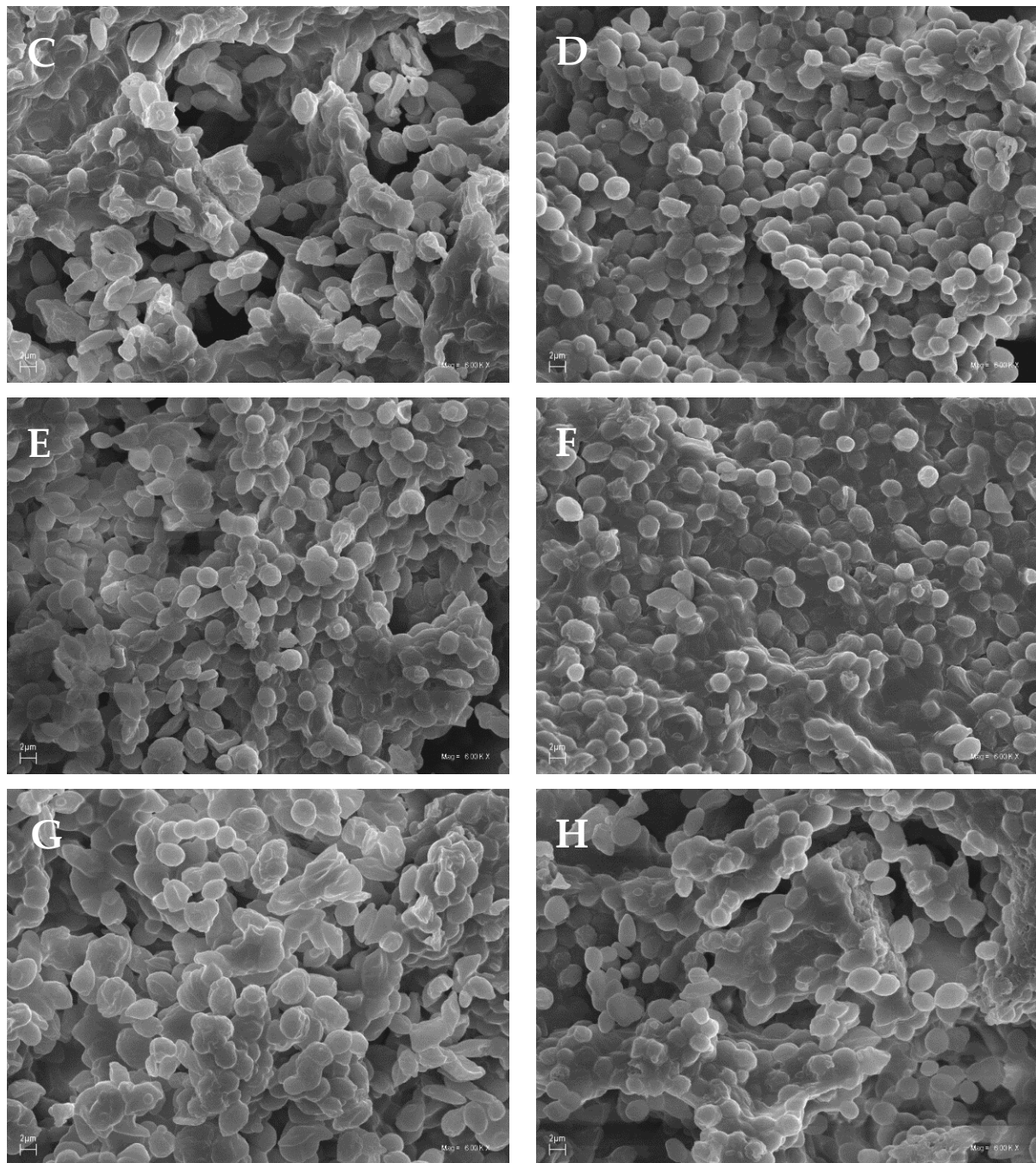


**Figure 1.** Effect of yeast cell pre-treatment on encapsulation yield. Statistically significant differences were marked by \* (comparing NY with ay).



**Figure 2.** Cont.

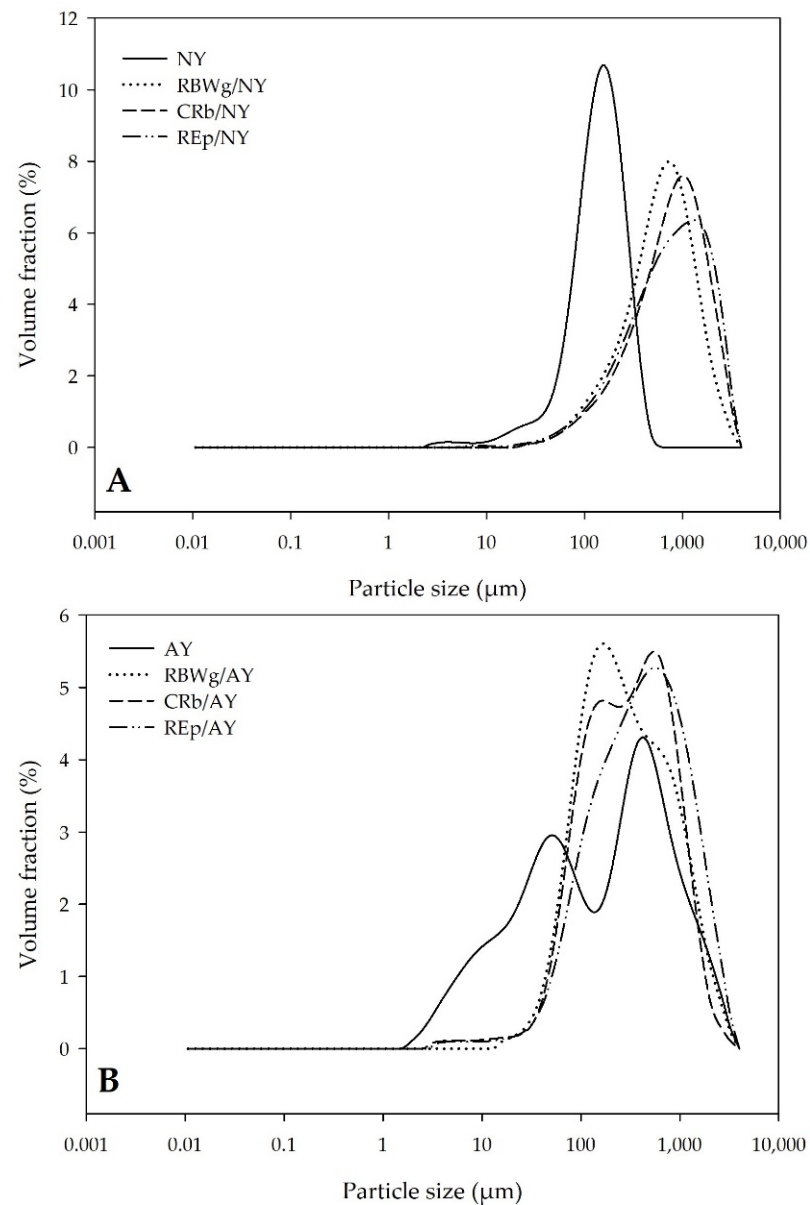




**Figure 2.** Scanning electron microscopic images of NY (A), AY (B), RBWg/NY (C), RBWg/AY (D), CRb/NY (E), CRb/AY (F), REp/NY (G), and REp/AY (H).

**Table 3.** YBMCs size distribution in μm.

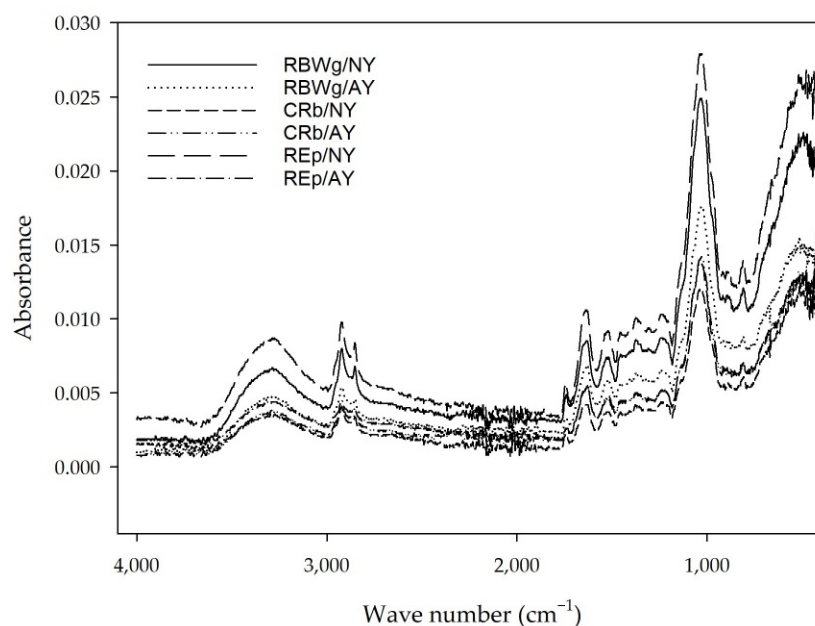
Oil Blends	NY			AY		
	Dx (10)	Dx (50)	Dx (90)	Dx (10)	Dx (50)	Dx (90)
RBWg	170.98 ± 11.18	621.03 ± 55.68	1520.72 ± 184.96	77.70 ± 2.30	261.86 ± 22.27	1133.33 ± 207.75
CRb	197.34 ± 11.11	798.88 ± 69.90	1958.45 ± 126.62	77.56 ± 1.63	305.88 ± 22.25	1033.61 ± 127.78
REp	172.72 ± 17.01	780.38 ± 79.21	2134.76 ± 150.17	88.75 ± 4.03	409.83 ± 40.75	1743.94 ± 230.84



**Figure 3.** Particle size distribution of NY-based (A) and AY-based (B) YBMCs.

### 3.4. FT-IR Analysis

The changes in the functional groups of the microcapsules were analyzed by FT-IR spectroscopy. It was previously proven that FT-IR microspectroscopy in the ATR mode can successfully study the composition of the global cell wall due to the reduced depth of penetration of the photon beam [50]. The spectra of the resulting changes are shown in Figure 4. The absorption spectra of the YBMCs showed no significant changes resulting from the content of various oil blends. A characteristic absorption band was observed at wave numbers  $3400\text{ cm}^{-1}$  and  $2900\text{ cm}^{-1}$ , responsible for the OH vibration bands of yeast and the asymmetric  $\text{CH}_2$  stretching vibrations of lipids [19,51]. Absorption maxima were recorded at the wave number  $1600\text{ cm}^{-1}$ , which corresponds to amide I and amide II bands in proteins, and the  $1050\text{ cm}^{-1}$   $\beta$ -1,3-glucans absorption band [52]. FT-IR analysis also showed a band related to the COO stretching vibration of triglycerides at  $1742\text{ cm}^{-1}$  [51].



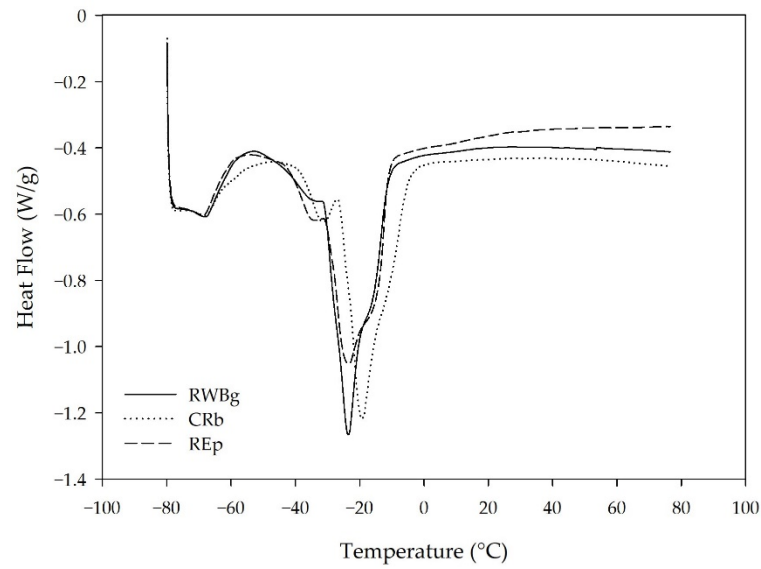
**Figure 4.** FT-IR spectra of capsules.

### 3.5. Thermal Oxidative Stability of YBMCs

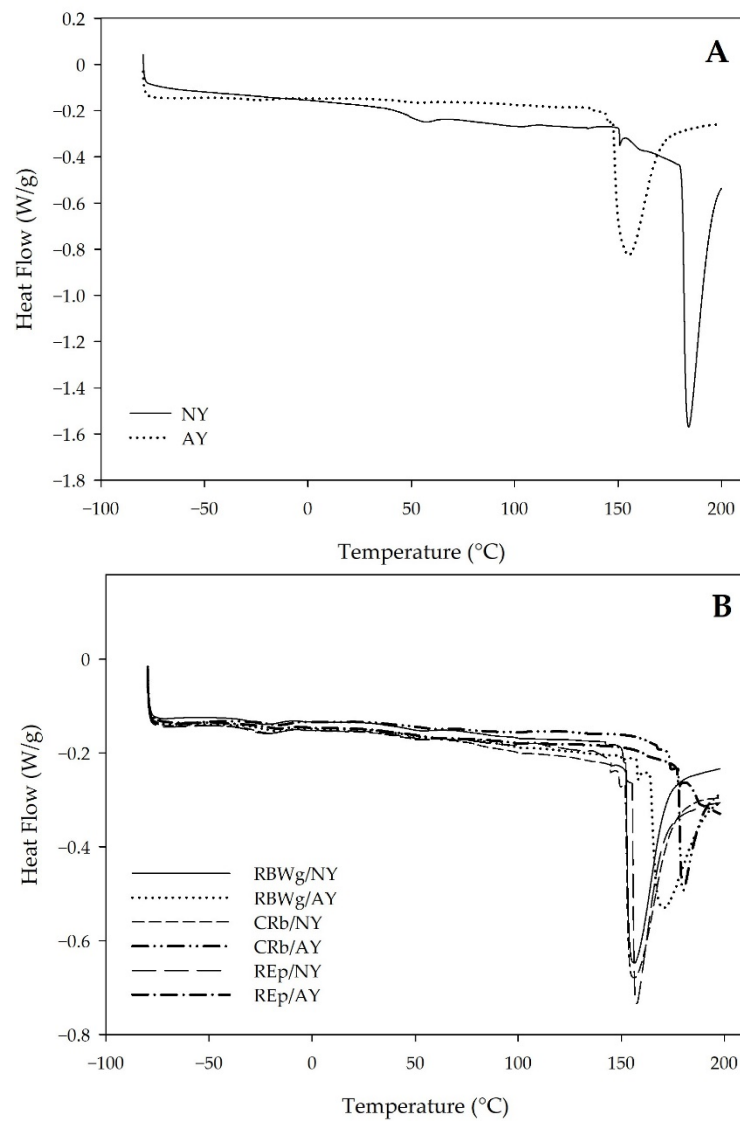
Oil blends with a  $\omega 3/\omega 6$  ratio of 5:1 are characterized by a large amount of unsaturated fatty acids (the sum of MUFA and PUFA is about 90%) and thus are very susceptible to oxidation. Many different factors affect oxidative stability, including resistance to oxidation caused by atmospheric oxygen, temperature, light, metal ions, etc. In these tests, the oxidative stability of the oil blends and the plasmolyzed and non-plasmolyzed YBMCs within the oils were assessed by DSC and TG measurements.

The high content of unsaturated fatty acids determined by chromatography (Table 2) within the oil blends used for encapsulation was confirmed by the curves of the softening characteristics of oils, determined by the DSC method (Figure 5). According to the literature data, the low temperatures of endothermic peaks are responsible for PUFA, and their content is higher in relation to the lower value of the endothermic recorded during the analysis [53,54]. The DSC melting curves of edible fats have different peak temperatures. Triacylglycerols containing unsaturated fatty acids in their structure are characterized by negative maximum peak temperatures (Figure 5). It proves the content of MUFA and PUFA in triacylglycerols of the tested oils [55]. In Figure 5, no endothermic peaks were observed; the maximum temperature would have had positive temperature values.

The DSC curves of native and autolyzed yeast (Figure 6A) indicate that NY shows an endothermic peak at about 61 °C, corresponding to the phase transition temperature of yeast cell phospholipid bilayers. The phase transition temperature of yeast depends on many factors, such as the temperature during their breeding, the microbiological medium used, or the method of aeration of the culture, but it depends also on the growth phase in which the yeast was collected and in the published works of other authors, different values were assumed [19,43]. In contrast to NY, AY, due to the liquefaction of the cell membrane caused by the autolysis process, saw only a slight phase transition at a temperature of about 55 °C, which is consistent with the decrease in this temperature after yeast cell lysis, described by other authors [51]. The encapsulation of oils in yeast cells is evidenced by small peaks with maxima in negative temperatures (Figure 6B). In the yeast figures, small endothermic peaks are present only for NY yeast, with positive temperatures of about 50 °C (Figure 6A). The presence of this peak may indicate the degradation of proteins (peptides). The peaks of temperature, which are in the range of positive temperatures, indicate the melting of carbohydrates.



**Figure 5.** DSC melting curves of oil blends used in encapsulation process.



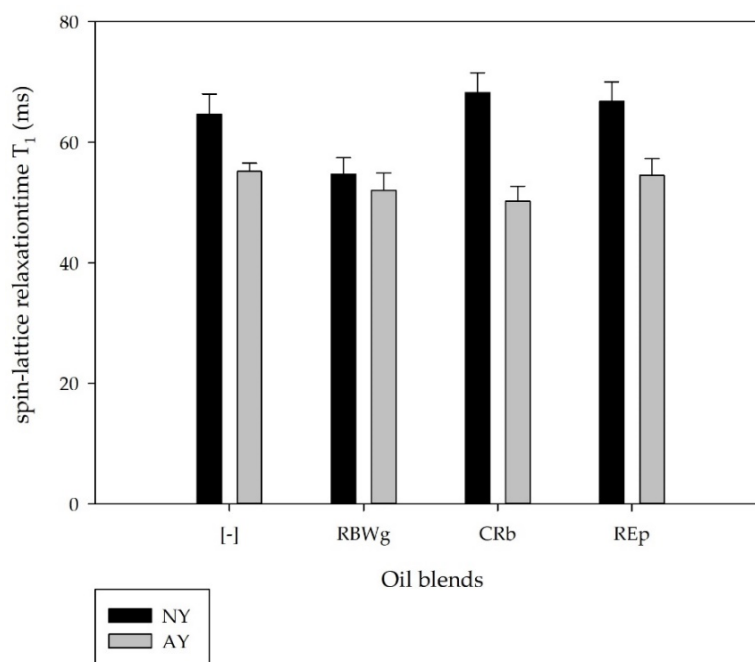
**Figure 6.** DSC curves of empty NY and AY (A), as well as YBMCs (B).

Changes in the course of the DSC curves for NY-based YBMCs are more pronounced. Endothermic peaks characterized by maximum temperatures at sub-zero temperatures indicate the presence of oils in the yeast capsules. In addition, the temperature values confirm the presence of triacylglycerol, the structure of which contains mono and polyunsaturated fatty acids. A decrease in the temperature of the endothermic reaction was observed, which may result from the integration of the encapsulated oil with the yeast bivalent lipid, which led to an easier transition from the gel to the liquid crystal state. van der Waals interactions between the oils and the cell membrane led to the reduction of its cohesiveness and, consequently, to its liquefaction [19]. At the same time, in the case of AY without and with encapsulated oils, an endothermic peak shift towards higher temperatures was demonstrated. As indicated by Kavosi et al. [51], such changes may indicate an increase in the thermal stability of the encapsulated oil.

### 3.6. Water Activity and LF NMR Relaxometry

The NY and AY trials showed  $a_w$  values of  $0.2741 \pm 0.0001$  and  $0.1660 \pm 0.0001$ , respectively. Measurements of water activity carried out for the YBMCs showed different values of  $a_w$  in the measuring chamber, which made it impossible to unambiguously characterize the value of this parameter. This means that there is no water available for the YBMCs to show any possibility of evacuation. All the water is trapped in the YBMCs structure.

LF NMR is a method used in food analysis since the 1990s [56–59]. It is a fast and accurate alternative to the use of drying and solvent extraction for determining the fat and moisture content of a biological system and is particularly suitable for the analysis of complex systems such as food products [60,61]. It involves measurements of the relaxation time of spin-lattice  $T_1$  and spin-spin  $T_2$ . Both parameters characterize the molecular dynamics of oil and water protons in the tested sample. Changes in their values reflect the relative changes in bulk water relative to bound water ( $T_1$ ) or describe the molecular dynamics of protons fractions. The analysis of the molecular dynamics of water in the tests, carried out by LF NMR methodology, showed that in NY and AY, significant differences had occurred for the values of spin-lattice relaxation times  $T_1$  (Figure 7). The spin-lattice  $T_1$  relaxation times for the YBMCs obtained from NY are longer, which may indicate a greater ordering of molecules containing protons [62,63].

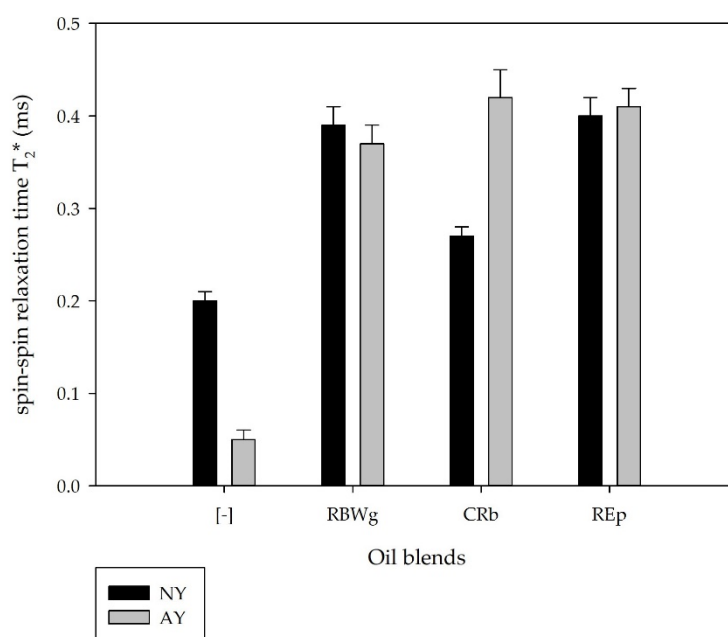


**Figure 7.**  $T_1$  relaxation time values.



As in the case of changes in  $a_w$ , higher values were found in all NY samples, which means greater mobility of water molecules. Plasmolysis removed the internal yeast organelles and thus facilitated the encapsulation of the oil, hence the lower  $T_1$  time value. Better encapsulation is also evidenced by the lower thermodynamic changes observed in the DSC analysis (see Section 3.5). Comparison of the  $T_1$  values for the YBMCs showed that the largest (26%) difference between the NY and AY trials was recorded for CRb, and the lowest (5%) for RBWg.

The values of spin-spin  $T_2^*$  times, presented in Figure 8, were also analyzed by using the shape of the free induction decay (FID) signals. YBMC samples containing oils are characterized by signals that are exponentially decaying. This exponentially decaying signal comes from the mobile liquid protons fraction. Thus, the results indicate that these relaxation time signals come only from the encapsulated oil, as confirmed by the results from the DSC.



**Figure 8.**  $T_2^*$  relaxation time values.

Additionally, when analyzing the shape of the FID signals (Figure S1), it was found that only NY and AY were characterized by two times  $T_2^*$ , described by the Gaussian curve and the exponential curve [64,65]. The Gaussian function comes from the solid proton fraction. In combination with the  $a_w$  results, a very short  $T_2^*$  time of 0.03 ms for NY and 0.05 ms for AY can be attributed to the unstructured water molecule. No water activity was recorded in the YBMCs; therefore, it should be concluded that the exponential components of the  $T_2^*$  times are the result of the relaxation of the protons of the structural components of oil.

#### 4. Conclusions

Microcapsules from new blends of oils with a favorable fatty acid profile were successfully prepared via a yeast-based microencapsulation process. The conducted research allows us to conclude that NY is a less efficient material for the oil encapsulation process. Earlier plasmolysis of yeast cells significantly improves the efficiency of the process. Moreover, importantly, YBMCs obtained from AY are characterized by lower aggregation, positively influencing their application value in food technology. The use of the encapsulation process resulted in the reduction of the oxidative changes of the encapsulated oils observed during thermal treatment, especially in YBMCs from autolyzed yeast; therefore, it is possible to effectively protect them in yeast capsules. More research on YBMC digestion, oil release, and in vitro and in vivo biological activity would be useful, which would show

whether the encapsulation process also maintains the activity of the compounds with beneficial pro-health effects present in cold-pressed oils.

## 5. Patent

The results presented in this article were used to prepare a patent application to The Patent Office of the Republic of Poland (patent application No. P.440018, dated 2021-12-29).

**Supplementary Materials:** The following supporting information can be downloaded at: <https://www.mdpi.com/article/10.3390/app12136577/s1>, Figure S1: Free induction decays (FIDs) of NY (A), AY (B), RBWg/NY (C), RBWg/AY (D), CRb/NY (E), CRb/AY (F), REp/NY (G) and REp/AY (H).

**Author Contributions:** Conceptualization, P.Ł.K.; Formal analysis, M.L. and P.Ł.K.; Investigation, W.C., A.C., K.S., P.J., H.M.B., K.W., E.O.-L. and P.Ł.K.; Methodology, D.K., H.M.B., E.O.-L. and P.Ł.K.; Project administration, M.L.; Resources, D.K. and P.Ł.K.; Supervision, P.Ł.K.; Visualization, W.C., M.B.R. and P.Ł.K.; Writing—original draft, W.C. and P.Ł.K.; Writing—review & editing, W.C., H.M.B., E.O.-L., M.B.R. and P.Ł.K. All authors have read and agreed to the published version of the manuscript.

**Funding:** The National Centre for Research and Development of Poland (NCBR) is acknowledged for the funding provided within the programme LIDER, under grant agreement No. LIDER/27/0105/L-11/19/NCBR/2020 (PI: Przemysław Kowalczewski).

**Institutional Review Board Statement:** Not applicable.

**Informed Consent Statement:** Not applicable.

**Data Availability Statement:** All data generated or analyzed during this study are included in this published article and its supplementary materials.

**Acknowledgments:** The authors thank Łukasz Masewicz (Department of Physics and Biophysics, Poznań University of Life Sciences, Poznań, Poland) for his help with the analyses.

**Conflicts of Interest:** The authors declare no conflict of interest. The funders had no role in the design of the study; in the collection, analyses, or interpretation of data; in the writing of the manuscript, or in the decision to publish the results.

## References

1. Calder, P.C.; Dangour, A.D.; Diekman, C.; Eilander, A.; Koletzko, B.; Meijer, G.W.; Mozaffarian, D.; Niinikoski, H.; Osendarp, S.J.M.; Pietinen, P.; et al. Essential fats for future health. Proceedings of the 9th Unilever Nutrition Symposium, 26–27 May 2010. *Eur. J. Clin. Nutr.* **2010**, *64*, S1–S13. [[CrossRef](#)] [[PubMed](#)]
2. Matthäus, B. Oil Technology. In *Technological Innovations in Major World Oil Crops, Volume 2*; Springer New York: New York, NY, USA, 2012; pp. 23–92.
3. Durazzo, A.; Fawzy Ramadan, M.; Lucarini, M. Cold Pressed Oils: A Green Source of Specialty Oils. *Front. Nutr.* **2022**, *8*, 836651. [[CrossRef](#)] [[PubMed](#)]
4. Chew, S.C. Cold-pressed rapeseed (*Brassica napus*) oil: Chemistry and functionality. *Food Res. Int.* **2020**, *131*, 108997. [[CrossRef](#)] [[PubMed](#)]
5. Tvrzicka, E.; Kremmyda, L.-S.; Stankova, B.; Zak, A. Fatty Acids as Biocompounds: Their Role in Human Metabolism, Health and Disease—A Review. Part 1: Classification, Dietary Sources and Biological Functions. *Biomed. Pap.* **2011**, *155*, 117–130. [[CrossRef](#)] [[PubMed](#)]
6. Grosshagauer, S.; Steinschaden, R.; Pignitter, M. Strategies to increase the oxidative stability of cold pressed oils. *LWT* **2019**, *106*, 72–77. [[CrossRef](#)]
7. Shahidi, F.; Zhong, Y. Lipid oxidation and improving the oxidative stability. *Chem. Soc. Rev.* **2010**, *39*, 4067. [[CrossRef](#)]
8. Laguerre, M.; Lecomte, J.; Villeneuve, P. Evaluation of the ability of antioxidants to counteract lipid oxidation: Existing methods, new trends and challenges. *Prog. Lipid Res.* **2007**, *46*, 244–282. [[CrossRef](#)]
9. Choe, E.; Min, D.B. Mechanisms and Factors for Edible Oil Oxidation. *Compr. Rev. Food Sci. Food Saf.* **2006**, *5*, 169–186. [[CrossRef](#)]
10. WHO; FAO. WHO and FAO Joint Consultation: Fats and Oils in Human Nutrition. *Nutr. Rev.* **2009**, *53*, 202–205. [[CrossRef](#)]
11. Kmiecik, D.; Fedko, M.; Siger, A.; Kowalczewski, P.Ł. Nutritional Quality and Oxidative Stability during Thermal Processing of Cold-Pressed Oil Blends with 5:1 Ratio of  $\omega 6/\omega 3$  Fatty Acids. *Foods* **2022**, *11*, 1081. [[CrossRef](#)]
12. Kmiecik, D.; Fedko, M.; Siger, A.; Kulczyński, B. Degradation of tocopherol molecules and its impact on the polymerization of triacylglycerols during heat treatment of oil. *Molecules* **2019**, *24*, 4555. [[CrossRef](#)] [[PubMed](#)]
13. Rudzińska, M.; Przybylski, R.; Wąsowicz, E. Products formed during thermo-oxidative degradation of phytosterols. *JAOCS J. Am. Oil Chem. Soc.* **2009**, *86*, 651–662. [[CrossRef](#)]

14. Fedko, M.; Kmiecik, D.; Siger, A.; Majcher, M. The Stability of Refined Rapeseed Oil Fortified by Cold-Pressed and Essential Black Cumin Oils under a Heating Treatment. *Molecules* **2022**, *27*, 2461. [[CrossRef](#)] [[PubMed](#)]
15. Márquez-Ruiz, G.; Ruiz-Méndez, M.V.; Velasco, J. Antioxidants in frying: Analysis and evaluation of efficacy. *Eur. J. Lipid Sci. Technol.* **2014**, *116*, 1441–1450. [[CrossRef](#)]
16. Karaca, A.C.; Nickerson, M.; Low, N.H. Microcapsule production employing chickpea or lentil protein isolates and maltodextrin: Physicochemical properties and oxidative protection of encapsulated flaxseed oil. *Food Chem.* **2013**, *139*, 448–457. [[CrossRef](#)]
17. Karrar, E.; Mahdi, A.A.; Sheth, S.; Mohamed Ahmed, I.A.; Manzoor, M.F.; Wei, W.; Wang, X. Effect of maltodextrin combination with gum arabic and whey protein isolate on the microencapsulation of gurun seed oil using a spray-drying method. *Int. J. Biol. Macromol.* **2021**, *171*, 208–216. [[CrossRef](#)]
18. Coradello, G.; Tirelli, N. Yeast Cells in Microencapsulation. General Features and Controlling Factors of the Encapsulation Process. *Molecules* **2021**, *26*, 3123. [[CrossRef](#)]
19. Paramera, E.I.; Konteles, S.J.; Karathanos, V.T. Microencapsulation of curcumin in cells of *Saccharomyces cerevisiae*. *Food Chem.* **2011**, *125*, 892–902. [[CrossRef](#)]
20. Kmiecik, D.; Fedko, M.; Kobus-Cisowska, J.; Kulczyński, B.; Przeor, M.; Szczepaniak, O.; Gramza-Michałowska, A. Cold-Pressed Oils Blends with Pro-Health and Technological Features. Polish Patent Application No. P.432047, 2 December 2019.
21. Kmiecik, D.; Fedko, M.; Kobus-Cisowska, J.; Kulczyński, B.; Przeor, M.; Gramza-Michałowska, A. Cold-pressed oils blends with pro-health and technological features. Polish Patent Application No. P.432048, 2 December 2019.
22. AOCS. Official Method Ce 1h-05. Determination of cis-, trans-, Saturated, Monounsaturated and Polyunsaturated Fatty Acids in Vegetable or Non-ruminant Animal Oils and Fats by Capillary GLC. *Off. Methods Recomm. Pract. Am. Oil Chem. Soc.* **2009**, *3*, 1–29.
23. Shi, G.; Rao, L.; Yu, H.; Xiang, H.; Pen, G.; Long, S.; Yang, C. Yeast-cell-based microencapsulation of chlorogenic acid as a water-soluble antioxidant. *J. Food Eng.* **2007**, *80*, 1060–1067. [[CrossRef](#)]
24. Czerniak, A.; Kubiak, P.; Białas, W.; Jankowski, T. Improvement of oxidative stability of menhaden fish oil by microencapsulation within biocapsules formed of yeast cells. *J. Food Eng.* **2015**, *167*, 2–11. [[CrossRef](#)]
25. Kowalczewski, P.Ł.; Czerniak, A.; Lesiecki, M.; Kmiecik, D.; Smarzyński, K. The Method of Encapsulation of Oils in Yeast Cells. Polish Patent Application No. P.440018, 29 December 2021.
26. Przybył, K.; Koszela, K.; Adamski, F.; Samborska, K.; Walkowiak, K.; Polarczyk, M. Deep and Machine Learning Using SEM, FTIR, and Texture Analysis to Detect Polysaccharide in Raspberry Powders. *Sensors* **2021**, *21*, 5823. [[CrossRef](#)] [[PubMed](#)]
27. Wirkowska, M.; Ostrowska-Ligeza, E.; Górka, A.; Koczoń, P. Thermal properties of fats extracted from powdered baby formulas. *J. Therm. Anal. Calorim.* **2012**, *110*, 137–143. [[CrossRef](#)]
28. Ostrowska-Ligeza, E.; Górka, A.; Wirkowska, M.; Koczoń, P. An assessment of various powdered baby formulas by conventional methods (DSC) or FT-IR spectroscopy. *J. Therm. Anal. Calorim.* **2012**, *110*, 465–471. [[CrossRef](#)]
29. Le Thanh-Blicharz, J.; Lewandowicz, J.; Małyszczak, Z.; Kowalczewski, P.Ł.; Walkowiak, K.; Masewicz, Ł.; Baranowska, H.M. Water Behavior of Aerogels Obtained from Chemically Modified Potato Starches during Hydration. *Foods* **2021**, *10*, 2724. [[CrossRef](#)]
30. Brosio, E.; Gianferri, R. Low-resolution NMR—An analytical tool in food characterization. In *Basic NMR in Food Characterization*; Brosio, E., Ed.; Research Signpost: Kerala, India, 2009; pp. 9–38.
31. Weglarz, W.P.; Haranczyk, H. Two-dimensional analysis of the nuclear relaxation function in the time domain: The program CracSpin. *J. Phys. D Appl. Phys.* **2000**, *33*, 1909–1920. [[CrossRef](#)]
32. Ratusz, K.; Symoniuk, E.; Wroniak, M.; Rudzińska, M. Bioactive Compounds, Nutritional Quality and Oxidative Stability of Cold-Pressed Camelina (*Camelina sativa* L.) Oils. *Appl. Sci.* **2018**, *8*, 2606. [[CrossRef](#)]
33. Young, K. Omega-6 (n-6) and omega-3 (n-3) fatty acids in tilapia and human health: A review. *Int. J. Food Sci. Nutr.* **2009**, *60*, 203–211. [[CrossRef](#)]
34. Blasi, F.; Montesano, D.; Simonetti, M.S.; Cossignani, L. A Simple and Rapid Extraction Method to Evaluate the Fatty Acid Composition and Nutritional Value of Goji Berry Lipid. *Food Anal. Methods* **2017**, *10*, 970–979. [[CrossRef](#)]
35. Simopoulos, A.P. The Importance of the Omega-6/Omega-3 Fatty Acid Ratio in Cardiovascular Disease and Other Chronic Diseases. *Exp. Biol. Med.* **2008**, *233*, 674–688. [[CrossRef](#)]
36. Barceló-Coblijn, G.; Murphy, E.J. Alpha-linolenic acid and its conversion to longer chain n-3 fatty acids: Benefits for human health and a role in maintaining tissue n-3 fatty acid levels. *Prog. Lipid Res.* **2009**, *48*, 355–374. [[CrossRef](#)] [[PubMed](#)]
37. Park, H.G.; Lawrence, P.; Engel, M.G.; Kothapalli, K.; Brenna, J.T. Metabolic fate of docosahexaenoic acid (DHA; 22:6 n-3) in human cells: Direct retroconversion of DHA to eicosapentaenoic acid (20:5 n-3) dominates over elongation to tetracosahexaenoic acid (24:6 n-3). *FEBS Lett.* **2016**, *590*, 3188–3194. [[CrossRef](#)] [[PubMed](#)]
38. Lee, H.; Woo, J.; Chen, Z.; Leung, S.; Peng, X. Serum fatty acid, lipid profile and dietary intake of Hong Kong Chinese omnivores and vegetarians. *Eur. J. Clin. Nutr.* **2000**, *54*, 768–773. [[CrossRef](#)] [[PubMed](#)]
39. Nikolić, M.; Jovanović, M.; Nikolić, K. Advantages and disadvantages of vegetarian nutrition. *Zdr. Zast.* **2019**, *48*, 51–56. [[CrossRef](#)]
40. Davis, B.C.; Kris-Etherton, P.M. Achieving optimal essential fatty acid status in vegetarians: Current knowledge and practical implications. *Am. J. Clin. Nutr.* **2003**, *78*, 640S–646S. [[CrossRef](#)]
41. Kilcher, G.; Delneri, D.; Duckham, C.; Tirelli, N. Probing (macro)molecular transport through cell walls. *Faraday Discuss.* **2008**, *139*, 199. [[CrossRef](#)]
42. Bishop, J.R.P.; Nelson, G.; Lamb, J. Microencapsulation in yeast cells. *J. Microencapsul.* **1998**, *15*, 761–773. [[CrossRef](#)]

43. Normand, V.; Dardelle, G.; Bouquerand, P.-E.; Nicolas, L.; Johnston, D.J. Flavor Encapsulation in Yeasts: Limonene Used as a Model System for Characterization of the Release Mechanism. *J. Agric. Food Chem.* **2005**, *53*, 7532–7543. [[CrossRef](#)]
44. Shi, G.; Rao, L.; Xie, Q.; Li, J.; Li, B.; Xiong, X. Characterization of yeast cells as a microencapsulation wall material by Fourier-transform infrared spectroscopy. *Vib. Spectrosc.* **2010**, *53*, 289–295. [[CrossRef](#)]
45. Pham-hoang, B.N.; Voilley, A.; Waché, Y. Molecule structural factors influencing the loading of flavoring compounds in a natural-preformed capsule: Yeast cells. *Colloids Surf. B Biointerfaces* **2016**, *148*, 220–228. [[CrossRef](#)]
46. Sultana, A.; Miyamoto, A.; Lan Hy, Q.; Tanaka, Y.; Fushimi, Y.; Yoshii, H. Microencapsulation of flavors by spray drying using *Saccharomyces cerevisiae*. *J. Food Eng.* **2017**, *199*, 36–41. [[CrossRef](#)]
47. Burgain, J.; Gaiani, C.; Linder, M.; Scher, J. Encapsulation of probiotic living cells: From laboratory scale to industrial applications. *J. Food Eng.* **2011**, *104*, 467–483. [[CrossRef](#)]
48. Zhao, R.; Sun, J.; Torley, P.; Wang, D.; Niu, S. Measurement of particle diameter of *Lactobacillus acidophilus* microcapsule by spray drying and analysis on its microstructure. *World J. Microbiol. Biotechnol.* **2008**, *24*, 1349–1354. [[CrossRef](#)]
49. Favaro-Trindade, C.S.; Santana, A.S.; Monterrey-Quintero, E.S.; Trindade, M.A.; Netto, F.M. The use of spray drying technology to reduce bitter taste of casein hydrolysate. *Food Hydrocoll.* **2010**, *24*, 336–340. [[CrossRef](#)]
50. Burattini, E.; Cavagna, M.; Dell’Anna, R.; Malvezzi Campeggi, F.; Monti, F.; Rossi, F.; Torriani, S. A FTIR microspectroscopy study of autolysis in cells of the wine yeast *Saccharomyces cerevisiae*. *Vib. Spectrosc.* **2008**, *47*, 139–147. [[CrossRef](#)]
51. Kavosi, M.; Mohammadi, A.; Shojae-Aliabadi, S.; Khaksar, R.; Hosseini, S.M. Characterization and oxidative stability of purslane seed oil microencapsulated in yeast cells biocapsules. *J. Sci. Food Agric.* **2018**, *98*, 2490–2497. [[CrossRef](#)]
52. Cavagna, M.; Dell’Anna, R.; Monti, F.; Rossi, F.; Torriani, S. Use of ATR-FTIR Microspectroscopy to Monitor Autolysis of *Saccharomyces cerevisiae* Cells in a Base Wine. *J. Agric. Food Chem.* **2010**, *58*, 39–45. [[CrossRef](#)]
53. Fasina, O.O.; Craig-Schmidt, M.; Colley, Z.; Hallman, H. Predicting melting characteristics of vegetable oils from fatty acid composition. *LWT-Food Sci. Technol.* **2008**, *41*, 1501–1505. [[CrossRef](#)]
54. Kaisersberger, E. DSC investigations of the thermal characterization of edible fats and oils. *Thermochim. Acta* **1989**, *151*, 83–90. [[CrossRef](#)]
55. Wirkowska-Wojdyła, M.; Ostrowska-Ligeza, E.; Górska, A.; Bryś, J. Application of Chromatographic and Thermal Methods to Study Fatty Acids Composition and Positional Distribution, Oxidation Kinetic Parameters and Melting Profile as Important Factors Characterizing Amaranth and Quinoa Oils. *Appl. Sci.* **2022**, *12*, 2166. [[CrossRef](#)]
56. Makowska, A.; Baranowska, H.M.; Michniewicz, J.; Chudy, S.; Kowalczewski, P.L. Triticale extrudates—Changes of macrostructure, mechanical properties and molecular water dynamics during hydration. *J. Cereal Sci.* **2017**, *74*, 250–255. [[CrossRef](#)]
57. Płowaś-Korus, I.; Masewicz, L.; Szewiel, A.; Rachocki, A.; Baranowska, H.M.; Medycki, W. A novel method of recognizing liquefied honey. *Food Chem.* **2018**, *245*, 885–889. [[CrossRef](#)] [[PubMed](#)]
58. Baranowska, H.M. Water Molecular Properties in Forcemeats and Finely Ground Sausages Containing Plant Fat. *Food Biophys.* **2011**, *6*, 133–137. [[CrossRef](#)]
59. Piątek, M.; Baranowska, H.M.; Krzywdzińska-Bartkowiak, M. Microstructure and water molecular dynamics in meat after thawing. *Fleischwirtschaft* **2013**, *93*, 100–104.
60. Ates, E.G.; Domenici, V.; Florek-Wojciechowska, M.; Gradišek, A.; Kruk, D.; Maltar-Strmečki, N.; Oztop, M.; Ozvural, E.B.; Rollet, A.-L. Field-dependent NMR relaxometry for Food Science: Applications and perspectives. *Trends Food Sci. Technol.* **2021**, *110*, 513–524. [[CrossRef](#)]
61. Kamal, T.; Cheng, S.; Khan, I.A.; Nawab, K.; Zhang, T.; Song, Y.; Wang, S.; Nadeem, M.; Riaz, M.; Khan, M.A.U.; et al. Potential uses of LF-NMR and MRI in the study of water dynamics and quality measurement of fruits and vegetables. *J. Food Process. Preserv.* **2019**, *43*, e14202. [[CrossRef](#)]
62. Goldman, M. Formal Theory of Spin–Lattice Relaxation. *J. Magn. Reson.* **2001**, *149*, 160–187. [[CrossRef](#)]
63. Torchia, D.; Szabo, A. Spin-lattice relaxation in solids. *J. Magn. Reson.* **1982**, *49*, 107–121. [[CrossRef](#)]
64. Neue, G. Simplification of dynamic NMR spectroscopy by wavelet transforms. *Solid State Nucl. Magn. Reson.* **1996**, *5*, 305–314. [[CrossRef](#)]
65. Derbyshire, W.; van den Bosch, M.; van Dusschoten, D.; MacNaughtan, W.; Farhat, I.A.; Hemminga, M.A.; Mitchell, J.R. Fitting of the beat pattern observed in NMR free-induction decay signals of concentrated carbohydrate–water solutions. *J. Magn. Reson.* **2004**, *168*, 278–283. [[CrossRef](#)]